

Electronic Raman scattering from $\text{La}_{0.7}\text{Sr}_{0.3}\text{MnO}_3$ exhibiting giant magnetoresistance

Rajeev Gupta and A. K. Sood*

Department of Physics, Indian Institute of Science, Bangalore, India 560 012

R. Mahesh and C. N. R. Rao

Solid State and Structural Chemistry Unit, Indian Institute of Science, Bangalore, India 560 012

(Received 8 July 1996)

Raman scattering experiments on metallic $\text{La}_{0.7}\text{Sr}_{0.3}\text{MnO}_3$ have been carried out using different excitation wavelengths as a function of temperature from 15 K to 300 K. Our data suggest a Raman mode attributed to electronic excitations centered at 2100 cm^{-1} whose intensity decreases with increasing temperature. If the Raman mode is attributed to single-particle excitation associated with the fluctuations of the mass tensor, the decreased intensity would then imply a reduction in the density of states at the Fermi energy with increasing temperature. [S0163-1829(96)07342-0]

Recent observations of colossal magnetoresistance have stimulated a renewed interest in the electronic properties of doped $\text{La}_{1-x}\text{A}_x\text{MnO}_{3-\delta}$ ($A = \text{Sr}, \text{Ba}, \text{Ca}, \text{Pb}$, and vacancies) and other transition metal oxides having strong electron correlations.¹ The rich phase diagram of $\text{La}_{1-x}\text{Sr}_x\text{MnO}_3$ shows a variety of phases like paramagnetic insulator, ferromagnetic metal, paramagnetic metal, spin-canted insulator, and ferromagnetic insulator as a function of doping x and temperature. For $0 < x < 0.2$, the materials are insulating at all temperatures and are antiferromagnetic or ferrimagnetic at low temperatures. In the range $0.2 < x < 0.5$ the system shows a temperature induced transition at $T_c(x)$ from the ferromagnetic metal at $T < T_c$ to a paramagnetic insulator. The end member ($x = 0$) is a charge transfer antiferromagnetic insulator having gap corresponding to the charge transfer excitation from oxygen $2p$ to a manganese $3d$ state. Out of the $(4-x)$ manganese d electrons, three electrons occupy the tightly bound d_{xy} , d_{yz} , and d_{xz} orbitals with very little hybridization with the oxygen $2p$ states and can be considered as a local spin S_c of $3/2$. The remaining $(1-x)$ electrons occupy the e_g state made of the $d_{x^2-y^2}$ and d_{z^2} orbitals and are strongly hybridized. There is a strong exchange interaction J_H (Hund's coupling) between the $3d$ t_{2g} local spin and the $3d$ e_g conduction electron. The e_g level is further split into $e_g^{1\uparrow}$ and $e_g^{2\uparrow}$ due to the Jahn-Teller (JT) effect. The $t_{2g}^{\uparrow}-e_g^{2\uparrow}$ and $e_g^{1\uparrow}-e_g^{1\downarrow}$ separation is about 2 eV as calculated by Satpathy *et al.* using the local spin density approximation.² The estimate of the JT split e_g band, namely, $e_g^{1\uparrow} - e_g^{2\uparrow} = 4E_0$, is 2.4 eV. It can, however, range from 0.4 eV to 4 eV as argued by Millis.³

The metal-insulator transition in the intermediate doping range is qualitatively understood using the Zener's "double-exchange" (DEX) model, in which the e_g electron hopping from site i to j must go with its spin parallel to S_c^i to its spin parallel to S_c^j . Millis *et al.*⁴ have shown that DEX alone cannot explain many aspects like the low transition temperature T_c and the large resistivity of $T > T_c$ phase or the sudden drop in resistivity below T_c . They have proposed that, in addition to DEX, there is a strong electron phonon coupling such that the slowly fluctuating local Jahn-Teller distortions

localize the conduction band electrons as polarons. As the temperature is lowered, the effective hopping matrix element t_{eff} characterizing the electron itineracy increases and the ratio of JT self-trapping energy E_{JT} to t_{eff} decreases. The JT distortion has to be dynamic because a static JT effect would cause a substantial distortion of the structure and the material would be antiferromagnetic. Coey *et al.*⁵ have argued from the experimental magnetoresistance data that for $T < T_c$, the e_g electrons are delocalized on an atomic scale but the spatial fluctuations in the Coulomb and spin-dependent potentials tend to localize the e_g electrons in wave packets larger than the Mn-Mn distance. It has also been noted^{5,6} that doped manganites are unusual metals, having resistivities greater than the maximum Mott resistivity (1–10 m Ω cm) and a very low density of states at the Fermi level.⁷

Optical conductivity measurements on $\text{La}_{0.825}\text{Sr}_{0.175}\text{MnO}_3$ as a function of temperature by Okimoto *et al.*⁸ in the range 0–10 eV show a band at ~ 1.5 eV and spectral weight is transferred from this band to low energies with decreasing temperature. This band at ~ 1.5 eV has been interpreted due to the interband transitions between the exchange-split spin-polarized e_g bands. At $T < T_c$, the conductivity spectrum is dominated by intraband transitions in the e_g band. A similar feature at ~ 1 eV has been observed in $\text{Nd}_{0.7}\text{Sr}_{0.3}\text{MnO}_3$ which shifts to lower energies with decreasing temperature which is argued to be consistent by taking into account the dynamic JT effect.⁹ There is no reported work on Raman scattering in these systems. Millis³ has suggested that the transition between the e_g levels split by the JT interaction can be Raman active. The electronic Raman scattering can be observed from the single-particle and collective plasmon excitations. The crystal structure with space group $R\bar{3}c$ (D_{3d}^6) with two formulas in the unit cell has A_{1g} and $4E_g$ Raman-active modes. Our objective was to study vibrational and electronic Raman scattering in doped manganites as a function of temperature. In this paper we report electronic Raman scattering from doped $\text{La}_{1-x}\text{Sr}_x\text{MnO}_3$ ($x = 0.3$) from 15 K to 300 K.

Polycrystalline pellets of $\text{La}_{0.7}\text{Sr}_{0.3}\text{MnO}_3$ prepared by citrate-gel route and sintered at 1473 K with an average grain size of ~ 3.5 μm were used.¹⁰ The samples on which detailed studies were done have a resistivity of 0.4 m Ω cm at

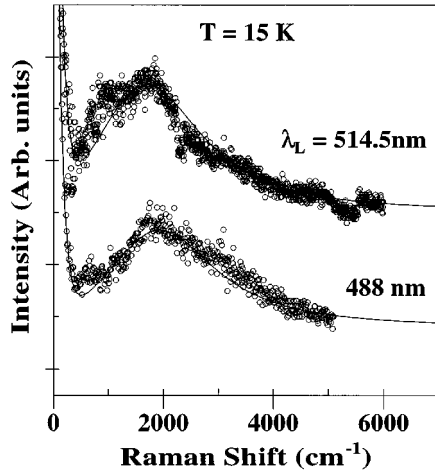


FIG. 1. Raman spectra recorded with different excitation wavelengths 514.5 nm and 488 nm at 15 K. The solid lines show the fitted function $[\text{Im}(-1/\epsilon)]$ to the data shown by open circles.

15 K and $3.5 \text{ m}\Omega \text{ cm}$ at 300 K. It shows a phase transition from a ferromagnetic metal to a paramagnetic insulator at $T_c \sim 380 \text{ K}$. The Raman measurements were carried out in the spectral range of $200\text{--}6000 \text{ cm}^{-1}$, at different temperatures from 15 K to 300 K. The spectra were recorded in the back scattering geometry using Spex Ramalog with photon counting detector (photomultiplier tube RCA C 31034 with GaAs cathode) using 514.5 nm and 488 nm lines of an argon ion laser (power density of $\sim 1500 \text{ W cm}^{-2}$ at the sample). The spectra have not been corrected for the spectrometer response. Pellets of thickness $\sim 2 \text{ mm}$ were mounted on the copper cold finger of the closed-cycle helium refrigerator (RMC model 22C CRYODYNE) using thermally cycled GE (M/s. General Electric) varnish. The temperature of the cold finger was measured using a platinum 100 sensor coupled to a home made temperature controller. The temperatures quoted are those of the cold finger and were measured to within a accuracy of $\sim 2 \text{ K}$. The experiments were done on three differently prepared pellets of $\text{La}_{0.7}\text{Sr}_{0.3}\text{MnO}_3$ and the results were similar to the ones reported here.

Figure 1 shows the recorded spectra at 15 K for the two different excitation wavelengths λ_L of 514.5 and 488 nm. Figure 2 shows the spectra recorded at different temperatures using the excitation wavelength of 488 nm. The spectrum was featureless at room temperature and hence is not shown. A small hump at $\sim 1000 \text{ cm}^{-1}$ in the spectrum recorded using 514.5 nm radiation is perhaps due to the spectrometer response. We have not been able to observe Raman scattering from the phonons. This may be due to the fact that the deviations from the cubic structure are rather small (optic phonon modes in perovskite structure with cubic symmetry of O_h^1 are not Raman active).

Inelastic light scattering can occur from single-particle or collective excitations (plasmons) of free carriers in metals and heavily doped (degenerate) semiconductors. The single-particle excitations corresponding to the charge density fluctuations in metals and semiconductors with a single sheeted Fermi surface are screened at low frequencies in a self-consistent manner by the carriers themselves.^{11,12} Thus, in simple free-electron-like carrier systems, light scattering

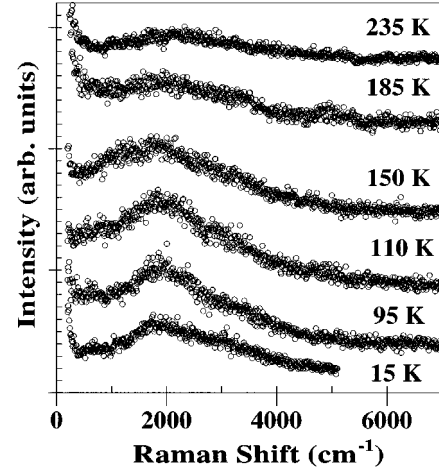


FIG. 2. Raman spectra at different temperatures using 488 nm excitation wavelength. Note that the intensity of the mode decreases as temperature increases.

from these single-particle excitations is not observed and only a peak at the plasma frequency can be seen. However, in a system with anisotropic Fermi surface like in a multi-valley semiconductor, charge density fluctuations in various equivalent valleys can be out of phase and exactly cancel others. These excitations do not carry any net charge and hence are not screened by the carriers. These excitations produce fluctuations of the mass tensor resulting in low-frequency Lorentzian-like line shape. The theory proposed by Ipatova *et al.*¹³ based on the collision-dominated electronic transport due to strong scattering of carriers by the impurities can explain the observed Raman scattering due to mass tensor fluctuations in *n*-type Si,¹⁴ *n*-type Ge,¹⁵ and high-temperature superconductors.¹⁶ In this theory the Raman scattering cross section is given by

$$I(\omega) = [n(\omega, T) + 1] \frac{B\omega\Gamma}{(\omega^2 + \Gamma^2)}, \quad (1)$$

where Γ is the scattering rate and

$$B = \frac{e^4}{\pi c^4} N(\epsilon_F) \left\langle \left| \hat{e}_L \left(\frac{\partial^2 \epsilon_{k\alpha}}{\partial \mathbf{k} \partial \mathbf{k}} - \left\langle \frac{\partial^2 \epsilon_{k\alpha}}{\partial \mathbf{k} \partial \mathbf{k}} \right\rangle \right) \hat{e}_S \right|^2 \right\rangle. \quad (2)$$

Here $\epsilon_{k\alpha}$ is the energy of the electron in band α with the momentum $\hbar \vec{k}$ and $N(\epsilon_F)$ the density of states at the Fermi level per unit volume. \hat{e}_L (\hat{e}_S) is the polarization of the incident (scattered) radiation. The brackets $\langle \rangle$ denote the Fermi surface average, $\langle f_k \rangle \equiv \sum_{k\alpha} f_k \delta(\epsilon_F - \epsilon_{k\alpha}) / \sum_{k\alpha} \delta(\epsilon_F - \epsilon_{k\alpha})$. Equation (2) can also be rewritten in terms of the effective mass tensor,

$$B = \frac{e^4}{\pi c^4} N(\epsilon_F) \langle |\hat{e}_L (\tilde{m}^{-1} - \langle \tilde{m}^{-1} \rangle) \hat{e}_S|^2 \rangle. \quad (3)$$

The term $[n(\omega, T) + 1]$ in Eq. (1) is the usual Bose-Einstein population factor. In Fermi liquid theory, Γ is frequency dependent and is taken to be $\Gamma(\omega) = \Gamma_0 + \alpha\omega^2$. The parameter α depends on the electron correlation effects and relates to the enhancement of the effective mass of the carriers. Equation (1) exhibits a maximum at $\omega \sim \Gamma_0$ and the peak

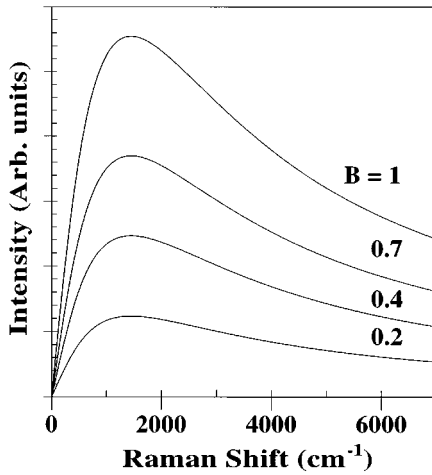


FIG. 3. Theoretical curves generated using Eq. (1) for different values of the scattering strength B .

intensity is proportional to B . Figure 3 shows a plot of Eq. (1) for different values of the strength parameter B , $\Gamma_0 = 2100 \text{ cm}^{-1}$, and $\alpha = 1 \times 10^{-3} \text{ cm}^{-1}$. The value of α is close to the value used¹⁷ to explain electronic Raman scattering in filling-controlled metals $\text{Sr}_{1-x}\text{La}_x\text{TiO}_3$. It can be seen that the plots in Fig. 3 are very similar to our observed Raman line shapes in Figs. 1 and 2. We have not fitted the data quantitatively to Eq. (1) because the signal-to-noise ratio of the data is not so high and the data is not corrected for the spectrometer response over the entire spectral range. The observed decrease of Raman peak intensity with increasing temperature implies that B and hence $N(\epsilon_F)$ decrease as the temperature is raised. The decrease of density of states at the Fermi energy with increasing T has been seen in photoemission studies⁷ and is argued to be related to the change in electron correlation strength U/W , where U is the effective Coulomb interaction strength and W is the d -band width. As T increases, U/W increases due to the combined effect of decreasing W as well as effective increase of U resulting from the decreasing degree of ferromagnetic order. The increase in U/W results in a transfer of single-particle spectral weight from the coherent features near ϵ_F to the incoherent part at higher energies.⁷

Another likely candidate for the observed Raman mode can be a collective electronic excitation, namely, the plasmon. At this stage without the data on the polarization selection rules on single-crystal samples, it is not possible to decide if the observed mode is associated with the single-particle excitation mentioned above or the plasmon. Raman scattering from the plasmon can be expressed by^{11,12}

$$I(\omega) = [n(\omega, T) + 1] \text{Im}[-1/\epsilon(\omega)], \quad (4)$$

where the dielectric function $\epsilon(\omega)$ can be (in the simplest Drude form) $\epsilon(\omega) = \epsilon_\infty [1 - \omega_p^2 / (\omega^2 + i\omega\Gamma_p)]$, ϵ_∞ is the high-frequency dielectric constant, ω_p is the plasma frequency, and Γ_p is the relaxation rate. The solid curves in Fig. 1 correspond to the best fit by Eq. (4) with parameters $\omega_p = 2100 \text{ cm}^{-1}$ and relaxation rate $\Gamma_p = 2600 \text{ cm}^{-1}$ (for spectra recorded using 514.5 nm radiation), and $\omega_p = 2300 \text{ cm}^{-1}$, $\Gamma_p = 2600 \text{ cm}^{-1}$ (for spectra recorded using 488 nm). Using $\omega_p^2 = 4\pi n_p e^2 / (\epsilon_\infty m^* m_e)$ where n_p is the number density of carriers of effective mass $m^* m_e$ (m_e is the mass of an electron), $\epsilon_\infty = 4.9$ (same¹⁸ as that of LaMnO_3), $n_p/m^* \sim 2.4 \times 10^{20} \text{ cm}^{-3}$. The number density calculated from the doping of 0.3 carriers per unit cell of cell volume⁶ 64 \AA^3 is $n_d = 5 \times 10^{21} \text{ cm}^{-3}$. Taking the effective mass of the carriers to be $m^* = 1$, it is seen that $n_p = 0.05 n_d$, i.e., the actual number of carriers is less than $(1-x)$ per manganese site. This can be related to the model of Coey *et al.*⁵ wherein the e_g electrons though delocalized on atomic scale are in magnetically localized wave packets spread over the Mn-Mn separation. If the localization energy of some carriers is less than $\hbar\omega_p$, they will not participate in the collective plasmon excitation. The localization of the carriers need not be as magnetic polarons but may involve lattice polarons as envisaged by Millis.^{3,4} The reduced number of carriers is consistent with the Hall measurements of Hundley as referred by Roder *et al.*¹⁹ The observed low density of states at Fermi energy⁷ also corroborates the less number of carriers deduced from ω_p . Perhaps m^* can be greater than 1 which will reduce the difference between the n_p and n_d . The dc resistivity in the free electron model is $\rho = m/n_p e^2 \tau$, where τ is the relaxation time of the carriers. Putting $\tau^{-1} = \Gamma_p$, ρ can be expressed in terms of ω_p^2 and Γ_p as $\rho = 4\pi\Gamma_p / (\epsilon_\infty \omega_p^2)$. Taking $\Gamma = 2600 \text{ cm}^{-1}$ and $\omega_p = 2100 \text{ cm}^{-1}$, we get $\rho = 7.2 \text{ m}\Omega \text{ cm}$, which is remarkably close to the measured values. The $\rho(T)$ and hence Γ increases with temperature and can therefore result in substantial reduction of Raman intensities, as seen in our experiments. The observed Raman frequency is much smaller than the estimated $4E_0$ and hence is not likely to be associated with the transition between the JT-split e_g bands.

In conclusion, we have observed Raman scattering from electronic excitations in the low-temperature metallic phase of $\text{La}_{0.7}\text{Sr}_{0.3}\text{MnO}_3$. Further polarized Raman experiments on these materials especially on single crystals can provide more clues as to the exact nature and symmetry of these excitations.

We thank Professor T.V. Ramakrishnan, R. Mahendiran, Professor A.K. Raychaudhuri, and Professor B.S. Shastry for useful discussions. A.K.S. thanks Department of Science and Technology, India and R.G. thanks CSIR for the financial assistance.

*Author to whom correspondence should be addressed. Electronic address: asood@physics.iisc.ernet.in

¹S. Jin, T.H. Tiefel, M. McCormack, R.A. Fastnacht, R. Ramesh, and L.H. Chen, *Science* **264**, 413 (1994).

²S. Satpathy, Z.S. Popovic, and F.R. Vukajlovic, *Phys. Rev. Lett.* **76**, 960 (1996).

³A.J. Millis (unpublished).

⁴A.J. Millis, P.B. Littlewood, and B.I. Shraiman, *Phys. Rev. Lett.* **74**, 5144 (1995).

⁵J.M.D. Coey, M. Viret, L. Ranno, and K. Ounadjela, *Phys. Rev. Lett.* **75**, 3910 (1995).

⁶R. Mahendiran, S.K. Tiwary, A.K. Raychaudhuri, T.V. Ramakrishnan, R. Mahesh, N. Rangavittal, and C.N.R. Rao, *Phys. Rev. B* **53**, 3348 (1996).

- ⁷D.D. Sarma, N. Shanti, S.R. Krishnakumar, T. Saitoh, T. Mizokawa, A. Sekiyama, K. Kobayashi, A. Fujimori, E. Weschke, R. Meier, G. Kaindl, Y. Takeda, and M. Takano, *Phys. Rev. B* **53**, 6873 (1996).
- ⁸Y. Okimoto, T. Katsufuji, T. Ishikawa, A. Urushibara, T. Arima, and Y. Tokura, *Phys. Rev. Lett.* **75**, 109 (1995).
- ⁹S.G. Kaplan, M. Quijada, H.D. Drew, D.B. Tanner, G.C. Xiong, R. Ramesh, C. Kwon, and T. Venkatesan, *Phys. Rev. Lett.* **77**, 2081 (1996).
- ¹⁰R. Mahendiran, R. Mahesh, A.K. Raychaudhuri, and C.N.R. Rao, *Solid State Commun.* **94**, 149 (1996).
- ¹¹M.V. Klein, in *Light Scattering in Solids*, edited by M. Cardona (Springer, Heidelberg, 1969), Vol. I, p. 147.
- ¹²G. Abstreiter, M. Cardona, and A. Pinczuk, *Light Scattering in Solids*, edited by M. Cardona and G. Guntherodt (Springer, Heidelberg, 1984), Vol. IV, p. 5.
- ¹³I.P. Ipatova, A.V. Subashiev, and V.A. Voitenko, *Solid State Commun.* **37**, 893 (1981).
- ¹⁴G. Contreas, A.K. Sood, and M. Cardona, *Phys. Rev. B* **32**, 924 (1985).
- ¹⁵G. Contreas, A.K. Sood, and M. Cardona, *Phys. Rev. B* **32**, 930 (1985).
- ¹⁶M.C. Krantz, I.I. Mazin, D.H. Leach, W.Y. Lee, and M. Cardona, *Phys. Rev. B* **51**, 5949 (1995).
- ¹⁷T. Katsufuji and Y. Tokura, *Phys. Rev. B* **49**, 4372 (1996).
- ¹⁸T. Arima and Y. Tokura, *J. Phys. Soc. Jpn.* **64**, 2488 (1995).
- ¹⁹H. Roder, J. Zang, and A.R. Bishop, *Phys. Rev. Lett.* **76**, 1356 (1996).